Non-equilibrium hybrid insertion/extraction through the 4th dimension in grand-canonical simulation

Luc Belloni

Non-equilibrium Hybrid Insertion/Extraction through the 4th Dimension in Grand-Canonical Simulation

Luc Belloni

LIONS, NIMBE, CEA, CNRS, Université Paris-Saclay, 91191-Gif-sur-Yvette, France

Abstract:

The process of inserting/deleting a particle during Grand-Canonical Monte-Carlo (MC) simulations is investigated using a novel, original technique: the trial event is made of a short non-equilibrium molecular dynamics (MD) trajectory during which a coordinate *w* along a 4th dimension is added to the particle in course of insertion/deletion and is forced to decrease from large values up to zero (for insertion) or increased from 0 up to large values (for extraction) at *imposed v_w* velocity. The probability of acceptation of the whole MC move is controlled by the chemical potential and the external work applied during the trajectory. Contrary to the standard procedures which create/delete *suddenly* a particle, the proposed technique gives time to the fluid environment to *relax* during the gradual insertion/extraction before acceptation decision. The reward for this expensive trial move is a gain of many orders of magnitude in success rate. The power and wide domain of interest of this hybrid "H4D" algorithm which marries stochastic MC and non-equilibrium deterministic MD flavors are briefly illustrated with hard sphere, water and electrolyte systems. The same approach can be easily adapted in order to *measure* the chemical potential of a solute particle immersed in a fluid during canonical or isobaric simulations. It then becomes an efficient application of the Jarzynski theorem for the determination of solvation free energy.

luc.belloni@cea.fr

Introduction

Within numerical simulations, the ability to *measure* or to *impose* the chemical potential (CP) μ provides valuable extra information. In the first case, the simulation is performed in *NVT* canonical or *NPT* isobaric conditions (*N* is the number of particles, *V* the volume, *T* the temperature and *P* the pressure) and the objective is the CP of an extra, solute particle. This may be a particle of the fluid itself when one wants to complete its equation of state $\mu(T,\rho)$ or $\mu(T,P)$ ($\rho=N/V$ is the number density) or is really a unique molecular/macromolecular solute immersed at infinite dilution in the bulk solvent in order to determine its excess CP μ^{exc} or solvation free energy. The fundamental Widom's insertion technique [1] creates *suddenly* a solute particle at random position inside a bulk solvent cell, calculates its experienced interaction potential v_{solute} and averages the Boltzmann factor $\beta\mu^{exc} = -\ln\left\langle e^{-\beta v_{solute}} \right\rangle_{solvent}$ ($\beta=1/kT$ is the inverse thermal energy). The inverse version starts from a solvent+solute simulation cell and follows the difference of energy induced by the sudden deletion of the solute, $\beta\mu^{exc} = +\ln\left\langle e^{\beta v_{solute}} \right\rangle_{solvent+solute}$. While formally exact, both techniques become rapidly inefficient in dense, cohesive systems where the interesting configurations which contribute the most to the averages are rarely if not never sampled. The Bennett's overlapping distribution technique [2] [3] which couples information from both simulations improves the precision but is still insufficient for multi-site solute molecules. So, a wide spectrum of theoretical approaches has been elaborated in the literature in order to circumvent this difficulty and calculate chemical potentials or free energy differences with great precision. They all share the use of "partial" solutes which interact with the solvent particles through a pair potential v_λ that interpolates *continuously* between $v_{\lambda=0}=0$ (no solute) and $v_{\lambda=1}=v$ (full solute, real potential v). Among the possible approaches [4], one briefly cites the thermodynamical integration and the free energy perturbation which require performing in parallel 20-40 simulations, each at a different intermediate fixed state λ. Other techniques treat λ as an extra degree of freedom, subject to a prescribed dynamics, and construct the potential of mean-force from the measured λ-distribution [5] [6]. Finally, the Jarzynski's approach [7] imposes a time-dependent law $\lambda(t)$ during a non-equilibrium simulation joining the two opposite states $\lambda=0$ and 1, and construct the CP from the external work W exerted on the solvent+partial solute system, $\beta\mu^{exc} = -\ln\left\langle e^{-\beta W} \right\rangle$.

In the second case, the simulation is performed in μVT Grand-Canonical (GC) ensemble which imposes the value of the solvent CP μ through exchanges of particles with a reservoir. This type of simulation is needed in heterogeneous interfacial or porous media in equilibrium with a bulk solvent. In homogeneous systems, it provides direct access to fundamental thermodynamical quantities from the particle number fluctuations $\langle\Delta N^2\rangle$ around the mean value $\langle N\rangle$. The repeated trial addition/subtraction of particles along the simulation suffers from the same difficulties as above: a trial random instantaneous insertion in a cell containing *N* particles will mainly conduct to an overlap and miss the interesting *N*+1 configurations, leading to a sure rejection. Inversely, a randomly chosen particle in the cell experiences a favorable (highly negative) energy inside its environment, not compatible with its sudden

deletion. The probability of acceptation is for instance 10^{-7} for a hard sphere fluid just below crystallization and less than 10^{-4} for a bulk water system. Admittedly, cavity-bias [8] and orientational-bias [4] techniques optimize the search for the very rare interesting locations for insertion or the very rare unhappy molecules for deletion and provide a reasonable increase in effective acceptation rate, but with known side-effects when the fluid has no time to relax between successive $N\pm1$ events [9]. The direct use of "partial" particles as above, with stochastic or deterministic λ trajectory [10] during the simulation, is not satisfactory here except if one accepts to explore the phase space with a non-integer, continuous N number in the cell.

Grand Canonical H4D algorithm

In the present work, we propose a different, new strategy for changing the particle number N. For a simple introduction, we ask the reader to think about the way a triangular rack is progressively filled with balls at the beginning of a billiards game: the balls can be considered as 2D disks which collide inside the horizontal, partially filled cell. How to add an extra ball? A standard naïve "GC" procedure would freeze a configuration and try to create *suddenly* a new disk at a 2D position on the plane, chosen randomly or in a biased fashion. The success would be obviously rather poor. On the other hand, the clear procedure in real life restores the 3D character of the balls, the extra one is pushed down from above the table *while* the horizontal fluid is *still* moving and the collisions in 3D space between all $N+1$ spheres guarantees the on-the-fly creation of a 2D cavity and relaxation of the fluid. With this simple picture in mind, we now return to the 3D GC numerical simulations: a coordinate w (say, $w\geq0$) along a 4$^{\text{th}}$ dimension [11][6], let us still call it the altitude, is added to the "flying" particle in course of insertion/deletion. A trial Monte-Carlo (MC) N change is made of a short Molecular Dynamics (MD) trajectory of the whole fluid performed under non-equilibrium conditions characterized by a time-dependent $w(t)$ *imposed* descent/ascent law. The external work needed to maintain this law from $w=+\infty/0$ up to $w=0/+\infty$ is combined with the imposed CP μ and monitors the probability of acceptation according to the GC MC recipe. Note that the use of a "partial" particle characterized by finite w which interpolates continuously between ideal and full coupling is here only transitory and limited to the trial MC event. Such type of "hybrid" [12], non-equilibrium MC-MD combination has already been used in the literature in order to favor giant steps and overcome energy barriers in canonical simulations [13][14][15]. We call our present strategy for GC particle exchanges "Hybrid 4 Dimension" or H4D. The details of the procedure are the following.

The 3D fluid molecules interact via site-site spherically symmetric pair potentials of the form $v_{ij}(r_{ij})$ where $r_{ij}=\left|\vec{r}_i-\vec{r}_j\right|$ is the ij separation. The configuration space is explored with standard MC translations/rotations. During a particle exchange with the reservoir, the interaction potentials become $v_{ij}\left(\sqrt{r_{ij}^2+(w_i-w_j)^2}\right)$ where the altitude w_i remains 0 for a site of the fluid and is w for a site of the flying particle at the altitude w. At the beginning of a trial insertion, the "old" configuration contains N particles with the total potential energy U_o. The GC weight of the configuration is $p_o\approx\frac{1}{N!}e^{N\beta\mu}e^{-\beta U_o}$. An extra particle is put at a random 3D position/orientation in the cell and at the finite altitude $w=w_{\max}>0$ (free). In case of molecules,

w_{max} is common to all sites. In case of flexible molecules, the intra configuration is drawn from the distribution in vacuum. w_{max} is the first of a long list of free parameters which can be chosen at will in order to optimize the efficiency of the technique. $w_{max}=0$ corresponds to the usual procedure with instantaneous creation. Too short values, say less than the site diameters, would provoke probable overlaps since the beginning. Too large values are unnecessary and would require very long MD trajectories. At time $t=0$, the N+1 3D old velocities $\vec{v}_i^{old}$ are drawn from the probability density $p_{insertion}(\vec{v}_i)$ (free). In all cases, we have chosen the natural Maxwell-Boltzmann distribution $p_{insertion}(\vec{v}_i) \approx \exp\left[-\dfrac{mv_i^2}{2kT}\right]$ where m is the mass. In $\sqrt{kT/m}$ units used in the following, the 3D velocities are of the order one. For rigid molecules, the angular velocities are drawn from similar distribution involving the inertia moments. Then, the 3D trajectory followed by the $N+1$ particles is provided by a non-equilibrium MD simulation during which the altitude w decreases with an imposed, constant $-v_w$ descent velocity ($v_w>0$, free). Again, $v_w=\infty$ corresponds to the standard creation process. The opposite limit $v_w \to 0$ would characterize a quasi-static insertion. For hard systems, the trajectory is made of successive elastic collisions in 4D space. For continuous potentials, the equations of motion are integrated with a finite time step Δt (free) and a time-reversible, area-preserving algorithm [16]. The N fluid particles are forced to stay always on the "horizontal" 3D space, $w=0$, thank to external "vertical" forces which do not produce work. The force field which controls the MD trajectory may derive from a simplified, degraded version (free) of the original potentials $v_{ij}(r)$ in order to speed up the calculations, like using shorter cut-offs in Ewald summations, at the risk of producing a final configuration not favorable for the true interaction. Once the flying particle has landed on the ground at $w=0$, the MD stops and the trial "new" ($N+1$) configuration is characterized by the velocities $\vec{v}_i^{new}$, the total potential energy U_n and weight $p_n \approx \dfrac{1}{(N+1)!}e^{(N+1)\beta\mu}e^{-\beta U_n}$. Inversely, a trial extraction from an old configuration starts by choosing randomly the future flying particle among the N fluid ones. The N 3D velocities are drawn from a probability density $p_{destruction}(\vec{v}_i)$ (free), again exclusively chosen here as the Maxwell-Boltzmann law. The non-equilibrium MD starts while the flying particle takes off from $w=0$ with the very same constant ascent velocity $+v_w$ and finishes when w reaches w_{max}, where the flying particle is finally entirely decoupled from the remaining $N-1$ fluid particles ($w=\infty$). The MD algorithm and the time step Δt are identical to those in the insertion process.

We are now ready to express the probability of acceptation of the trial particle exchange. The transition matrix from the old to the new configuration $\alpha(o \to n)$ depends only on the choice of the initial velocities since the MD is a deterministic process (and the algorithm conserves phase space volumes):

$$\alpha(o \to n) = \prod_{i=1}^{N+1/N} p_{ins/des}(\vec{v}_i^{old}) = e^{-\beta K_o} \qquad (1)$$

where K_o is the kinetic energy of the old configuration. Since the MD algorithm is time-reversible (in fact, one just requires that the two algorithms used during insertion and destruction for integrating the equations of motion are time-inverses one to each other), the inverse transition matrix which produces the old configuration from the new one reads:

$$\alpha(n \to o) = \prod_{i=1}^{N+1/N} p_{des/ins}(-\vec{v}_i^{\,new}) = e^{-\beta K_n} \qquad (2)$$

where K_n is the kinetic energy of the new configuration. According to the detailed balance condition [4], the Metropolis probability of acceptation of the trial particle exchange becomes finally:

$$
\begin{aligned}
acc(o \to n) &= \min\left(1, \frac{\alpha(n \to o)}{\alpha(o \to n)} \frac{p_n}{p_o}\right) \\
&= \min\left(1, \frac{aV}{N+1} e^{-\Delta H_{on}}\right) \quad \text{insertion} \\
&= \min\left(1, \frac{N}{aV} e^{-\Delta H_{on}}\right) \quad \text{destruction}
\end{aligned}
\qquad (3)
$$

where $a=e^{\beta\mu}$ represents the activity and $\Delta H_{on}=H_n-H_o$ is the change of the total mechanical energy $H=K+U$ from the old to the new configuration. In the present adiabatic H4D version where the trial non-equilibrium MD trajectory is produced without thermostat, there is no exchange of heat with the exterior and the change of total energy is equal to the external work W required to maintain fixed the vertical velocity v_w despite the numerous 4D collisions with the bulk. For continuous potentials, the equations of motion are not integrated exactly due to the finite Δt step and the strict equality $\Delta H_{on}=W$ does not hold. Nevertheless, the MC rule (3) always applies [17]. The only risk of choosing a too large Δt value in order to shorten the MD simulation is to produce too wild positive departures of ΔH_{on} and to automatically reduce the acceptation rate.

Compared to the standard procedure ($w_{max}=0$ or $v_w=\infty$, $\Delta H_{on}= \Delta U_{on}$), the described H4D new technique replaces a very cheap trial exchange (cost=1 particle energy evaluation) by a very expensive one (cost=$w_{max}/(v_w\Delta t)$ MD time steps for N particles). The reward is that the bulk environment has time to react to the smooth insertion/extraction process before acceptation decision and the success rate increases by orders of magnitude. Moreover, when the particle exchange has been accepted, the produced configuration is characteristic of the new N value (and does not belong to the far positive aisle of the energy spectrum as with the usual techniques) and the MD trajectory has not been waste of time because it has enabled to shuffle the whole cell. Three preliminary examples of application are briefly presented now. Technical details are given in the Supplementary Material (SM).

Hard-sphere fluid

For pure hard sphere systems (diameter=σ), the acceptation rate within the standard procedure is easily estimated from the last line of (3) and roughly equals the inverse activity

coefficient $1/\gamma=\rho/a=$ e$^{-\beta\mu exc}$. This explains why the GC equations of state $\mu(\rho)$ reported in the literature are limited to $\rho^*=\rho\sigma^3\approx0.7$-$0.8$ ($\gamma\approx10^3$-10^4) [18] [19], well below the fluid-crystal phase transition which appears at $\rho_F^*=0.94$, $\gamma\approx10^7$ [4]. On the other hand, the present H4D technique enables to cover the whole fluid range and even a large part of the metastable fluid branch beyond ρ_F^*, up to $\rho^*\approx1$ (53% volume fraction), see Figure 1. While the probability of acceptation of the standard technique falls off more than exponentially from 10^{-2} to 10^{-9} when ρ^* goes from 0.6 to 1, it only slightly decreases from 55% to 15% with the H4D parameters $w_{max}=\sigma$, $v_w\approx0.1$. An overlap is (almost) always experienced during insertion in the former case, while it never happens in the latter case. It is interesting to note that when ρ approaches ρ_F^*, the hard sphere system spontaneously switches between two "phases" of different densities, one fluid, the other crystallized! Above ρ_F^*, the crystal eventually wins.
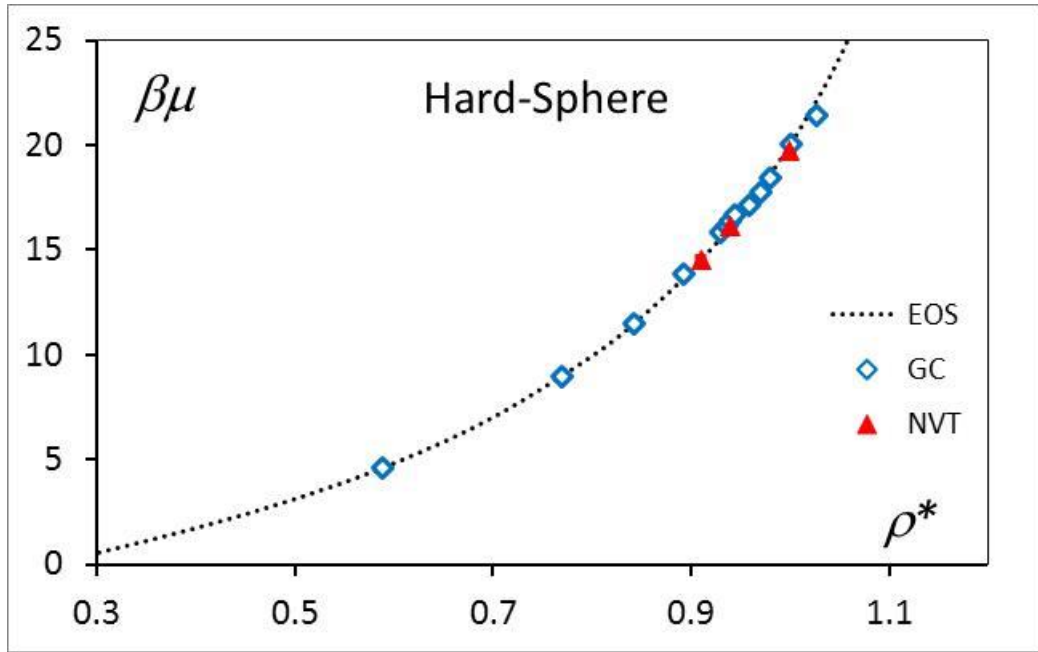

Figure 1: Chemical potential μ versus density ρ^* for the hard sphere system. The symbols refer to the present H4D technique ($w_{max}=\sigma$, $v_w=0.1$) used in GC (diamonds) or canonical (triangles) conditions. The cell size is $L=5\sigma$ for $\rho^*<0.9$ ($N\approx100$) and $L\approx6.3\sigma$ for $\rho^*>0.9$ ($N\approx235$). Dotted line: analytical equation of state of Hall [20].

Liquid water

The chemical potential of the popular SPC/E water model at room conditions has been recently measured with great precision using canonical, isobaric and standard GC Monte-Carlo simulations: $\mu=-15.37kT$ (where the activity a is expressed in Å^{-3}) [21]. We have repeated the GC simulation, this time using the H4D technique, see SM. Figure 2 presents the distributions $p_{ins}(\Delta M)$ and $p_{des}(\Delta M)$ of generalized energy change ΔM observed during the trial particle exchanges, where $\Delta M = \Delta H + kT\ln\dfrac{N+1}{V}$ for insertion and $-\Delta M = \Delta H + kT\ln\dfrac{V}{N}$ for destruction (ΔM is always count in the direction of insertion).

According to the Crooks theorem [22] (the non-equilibrium version of the Bennett's [2]), the two distributions verify:

$$p_{des}(\Delta M) = e^{\beta\mu} p_{ins}(\Delta M) e^{-\beta\Delta M} \tag{4}$$

and, in particular, cross at $\Delta M=\mu$. While the standard technique experiences very different energy transfers in the two directions (mainly excluded volume overlaps at insertion, highly negative cohesive energy at destruction), the two H4D distributions explore narrower, overlapped energy domains and take much higher values at the crossing point, see figure 2. As a consequence, the acceptation rate increases from 9 10^{-5} at $v_w=\infty$ up to 0.38 at $v_w=0.05$. An optimal compromise between N exchange success and speed of calculation is obtained with $v_w\approx0.2$ (14% success rate).
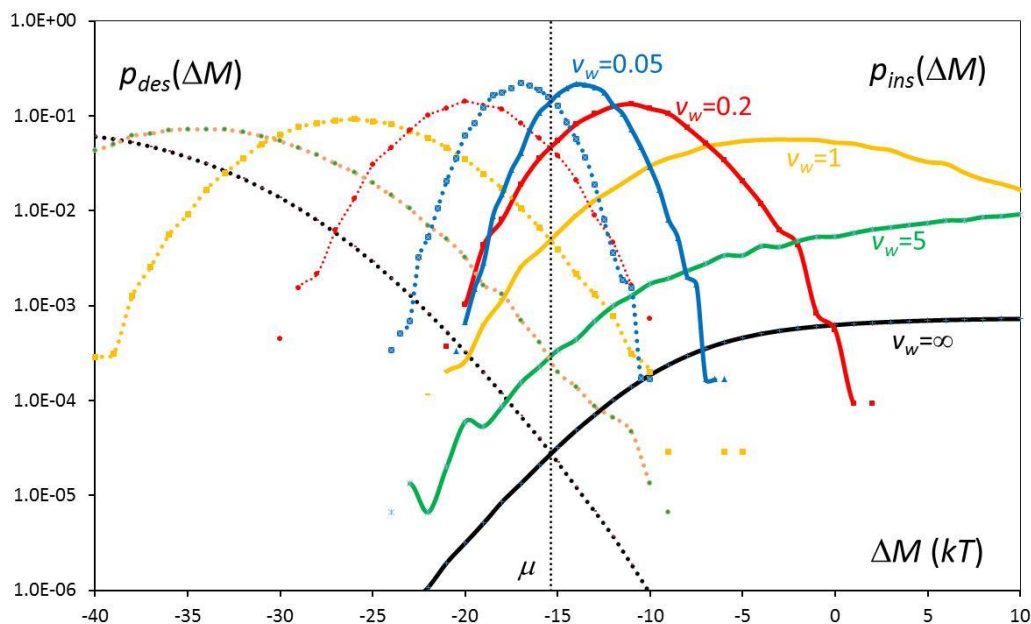

Figure 2: Distributions of generalized energy change ΔM observed during insertion (solid lines, right) and destruction (dotted lines, left) in GC simulation of SPC/E water system. Each curve is colored and labelled with the value of the vertical velocity v_w used in H4D procedure ($v_w=\infty$ corresponds to the usual technique). All insertion/destruction pairs cross at $\Delta M=\mu=-15.37kT$.

As an illuminating illustration, a video movie shows the MC/H4D procedure working for the insertion of a H_2O molecule into a 2D water layer using the 3rd dimension. Figure 3 presents a snapshot taken at $w=1$Å (Multimedia view).

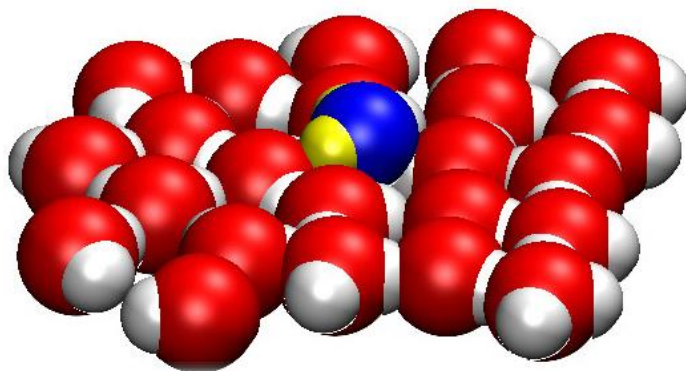*Figure 3: MC/H4D insertion of a H₂O molecule into a 2D water layer through the 3rd dimension. Snapshot taken at w=1Å. The video movie illustrates the on-the-fly reorganization of the H-bonding network in order to accommodate the extra molecule. A destruction event with gradual filling of the growing cavity left by the leaving particle simply corresponds to the inverse movie (Multimedia view).*

NaCl electrolyte

Lastly, we show how the H4D technique can be generalized for a Monte-Carlo simulation of NaCl aqueous electrolyte at the molecular solvent level of description, in the ensemble $N_{solvent}\mu_{salt}PT$. The number of SPC/E H₂O molecules is fixed, the volume fluctuates at the imposed pressure P=1bar and the number of ion pairs N_{Na+}=N_{Cl-}=N_{salt} varies through exchanges with a salt reservoir which imposes the chemical potential μ_{salt}=μ_{Na+}+μ_{Cl-}. To the author's knowledge, this is the very first time that a simulation investigates such type of ensembles with trial ion transfers in bulk water. The electrostatic coupling is strong, especially inside the solvation layers. Moreover, the process must involve the simultaneous insertion or destruction of *two* ions, one cation, one anion in order to preserve the electroneutrality. As a consequence, the trial transfer needs to operate very slowly, with a small vertical velocity, in order to reach reasonable acceptation rates, in the 1% range, and the computational cost is heavy. Nevertheless, the simulation of a 1M NaCl aqueous solution at room conditions has been successfully realized. The salt chemical potential has been first estimated from *measurements* during isobaric simulations (see below), μ_{salt}=-301.1kT. Then, the H4D-GCMC simulation has been performed with N_{H2O}=550 solvent molecules, w_{max}=3Å, v_w=0.0125 and special tricks, see SM for the details. The resulting ion number fluctuates around the average $<N_{salt}>$≈10.2 with a root mean square fluctuation $\sqrt{<\Delta N_{salt}^2>}$≈2.2. The mean densities are $<\rho_{salt}>$=1.01M, $<\rho_{H2O}>$=54.4M. The combination of volume + ion number exchanges in this two-component mixture is sufficient to account for total density *as well as* composition fluctuations, so for all cross partial density fluctuations, and the full Kirkwood-Buff theory applies [23]. For instance, the osmotic compressibility is given by:

$$\chi_{\text{osmotic}} = \left(\frac{\partial \rho_{\text{salt}}}{\partial \beta P_{\text{osmotic}}} \right)_{T, \mu_{\text{h}_{2o}}} = \langle V \rangle \frac{\langle \Delta \rho_{\text{salt}}^2 \rangle}{\langle \rho_{\text{salt}} \rangle} \tag{5}$$

and equals $\chi_{\text{osmotic}} \approx 0.45 \pm 0.03$ in the present 1M solution. At the same time, the radial pair distribution functions $g_{ij}(r)$ are *not* affected by the so-called explicit finite-size corrections so disturbing in the usual canonical or isobaric simulations of mixtures [24] [25], which result from the absence of fluctuations and prevent the direct determination of the Kirkwood-Buff integrals and thermodynamic derivatives. As an illustration, figure 4 plots the 3 "running" ion-ion structure factors $S_{ij}(R) = \delta_{ij} + \rho_{\text{salt}} \int_0^R (g_{ij}(r) - 1) d\vec{r}$. They all converge to the common asymptote χ_{osmotic} (the same value as above) in the present ensemble while they are useless (without special corrections) in the $N_i PT$ ensemble.

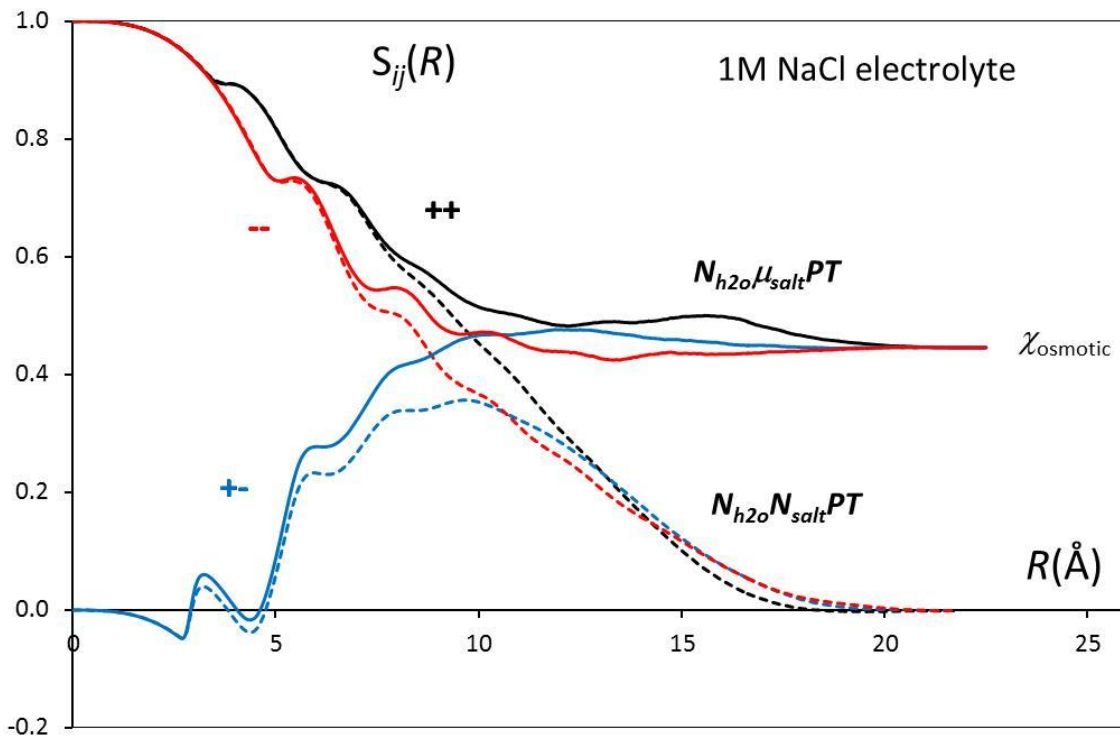*Figure 4: Running ion-ion structure factors $S_{ij}(R)$ in 1M NaCl electrolyte. MC simulation with $N_{H2O}=550$. Dashed lines: the number of ions is fixed, $N_{salt}=10$; Solid lines: N_{salt} fluctuates through H4D exchanges with a salt reservoir, $\beta\mu_{salt}=-301.1$.*

Canonical or isobaric H4D version

Up to now, the H4D technique has been described as a Grand-Canonical strategy for performing addition/subtraction of bulk fluid particles. It can be used as well for measuring the chemical potential or solvation free energy of a solute particle during canonical or isobaric simulations. The starting point considers the average of the Markov flux ratio:

$$\left\langle \frac{\alpha(n \to o)}{\alpha(o \to n)} \frac{p_n}{p_o} \right\rangle_o = \sum_o p_o \sum_n \alpha(o \to n) \left[\frac{\alpha(n \to o)}{\alpha(o \to n)} \frac{p_n}{p_o} \right]$$
$$= \sum_n p_n \sum_o \alpha(n \to o) = \sum_n p_n = 1 \tag{6}$$

From (3)(6), the CP of the fluid is thus given by:

$$\beta\mu = -\ln \left\langle \frac{V}{N+1} e^{-\beta\Delta H_{on}} \right\rangle_{ins} = -\ln \left\langle e^{-\beta\Delta M} \right\rangle_{ins} \quad \text{insertion}$$
$$= +\ln \left\langle \frac{N}{V} e^{-\beta\Delta H_{on}} \right\rangle_{des} = +\ln \left\langle e^{+\beta\Delta M} \right\rangle_{des} \quad \text{destruction} \tag{7}$$

These expressions, originally established in GC ensemble, can be used as well in canonical or isobaric conditions for *N* fixed to the averaged GC value (with the undesired presence of finite-size perturbations in the former case). For the hard sphere system, H4D-*NVT* data added in figure 1 nicely agree with the GC curve on the whole fluid branch.

Moreover, the same reasoning can be followed for a solvent+solute mixture at infinite dilution of the solute and the final expression for the solvation free energy of the solute reads:

$$\beta\mu_{solute}^{exc} = -\ln \left\langle e^{-\beta\Delta M} \right\rangle_{pure\,solvent} \quad \text{insertion}$$
$$= +\ln \left\langle e^{+\beta\Delta M} \right\rangle_{solvent+solute} \quad \text{destruction} \tag{8}$$

where $\Delta M = \Delta H_{on}$ for a H4D insertion of a solute inside a bulk solvent cell and $\Delta M = -\Delta H_{on}$ for a H4D extraction of the solute from a solvent+solute cell. This is nothing but an application of the Jarzynski's theorem. As usual, the combination of the insertion and destruction ΔM distribution data with the help of the Crooks theorem (4) and well-developed BAR techniques provide better statistic precision.

Conclusion

In this letter, we have introduced the bare version of the new H4D technique for efficient Grand-Canonical insertions/extractions which enables to treat otherwise unreachable new systems. The very same procedure helps in measuring the solvation free energy of solute molecules. The detailed application on various solvents, mixtures, solutes and the developments of more complex and optimized versions will be described in future papers.

References

1. B. Widom, J. Chem. Phys. **39**, 2808 (1963)

2. C. H. Bennett, J. Comput. Phys. **22**, 245 (1976)

3. K. S. Shing and K. E. Gubbins, Mol. Phys. **49**, 1121 (1983)

4. D. Frenkel and B. Smit. *Understanding Molecular Simulation;* Academic Press, 1996.

5. X. Kong and I. C.L. Brooks, J. Chem. Phys. **105**, 2414 (1996)

6. R. Pomès, E. Eisenmesser, C. B. Post, and B. Roux, J. Chem. Phys. **111**, 3387 (1999)

7. C. Jarzynski, Phys. Rev. Lett. **78**, 2690 (1997)

8. M. Mezei, Mol. Phys. **40**, 901 (1980)

9. J. C. Shelley and G. N. Patey, J. Chem. Phys. **102**, 7656 (1995)

10. T. Cagin and B. M. Pettitt, Mol. Phys. **72**, 169 (1991)

11. T. C. Beutler and W. F. van Gunsteren, J. Chem. Phys. **101**, 1417 (1994)

12. B. Mehling, D. W. Heermann, and B. M. Forrest, Phys. Rev. B **45**, 679 (1992)

13. H. A. Stern, J. Chem. Phys. **126**, 164112 (2007)

14. A. J. Ballard and C. Jarzynski, Proc. Natl. Acad. Sci.(USA) **106**, 12224 (2009)

15. Y. Chen and B. Roux, J. Chem. Phys. **141**, 114107 (2014)

16. N. Matubayasi and M. Nakahara, J. Chem. Phys. **110**, 3291 (1999)

17. Y. Chen and B. Roux, J. Chem. Phys. **142**, 024101 (2015)

18. D. J. Adams, Mol. Phys. **28**, 1241 (1974)

19. B.. F.D. Smit, J. Phys.: Condens. Matter **1**, 8659 (1989)

20. K. R. Hall, J. Chem. Phys. **57**, 2252 (1972)

21. L. Belloni, J. Chem. Phys. **149**, 094111 (2018)

22. G. E. Crooks, Phys. Rev. E **60**, 2721 (1999)

23. J. G. Kirkwood and F. P. Buff, J. Chem. Phys. **19**, 774 (1951)

24. A. Perera, L. Zoranic, S. Sokolic, and R. Mazighi, J. Mol. Liq. **159**, 52 (2011)

25. P. Krüger, S. K. Schnell, D. Bedeaux, S. Kjelstrup, T. J.H. Vlugt, and J. Simon, J. Phys. Chem. Lett. **4**, 235 (2013)